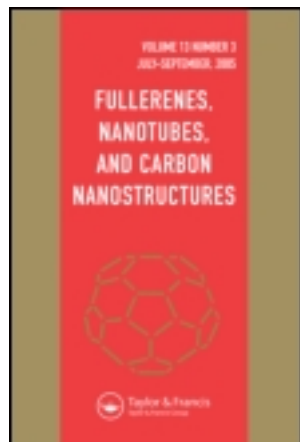


This article was downloaded by: [vali parvaneh]

On: 15 May 2012, At: 08:46

Publisher: Taylor & Francis

Informa Ltd Registered in England and Wales Registered Number: 1072954 Registered office: Mortimer House, 37-41 Mortimer Street, London W1T 3JH, UK



## Fullerenes, Nanotubes and Carbon Nanostructures

Publication details, including instructions for authors and subscription information:

<http://www.tandfonline.com/loi/lfn20>

### Torsional Buckling Behavior of SWCNTs Using a Molecular Structural Mechanics Approach Considering Vacancy Defects

Vali Parvaneh<sup>a</sup>, Mahmoud Shariati<sup>b</sup>, Hamid Torabi<sup>c</sup> & Amir Masood Majd Sabeti<sup>b</sup>

<sup>a</sup> Department of Engineering, Islamic Azad University, Shahrood Branch, Shahrood, Iran

<sup>b</sup> Department of Mechanical Engineering, Shahrood University of Technology, Shahrood, Iran

<sup>c</sup> Young Researchers' Club, Mashhad Branch, Islamic Azad University, Mashhad, Iran

Available online: 14 May 2012

To cite this article: Vali Parvaneh, Mahmoud Shariati, Hamid Torabi & Amir Masood Majd Sabeti (2012): Torsional Buckling Behavior of SWCNTs Using a Molecular Structural Mechanics Approach Considering Vacancy Defects, *Fullerenes, Nanotubes and Carbon Nanostructures*, 20:8, 709-720

To link to this article: <http://dx.doi.org/10.1080/1536383X.2011.572311>

PLEASE SCROLL DOWN FOR ARTICLE

Full terms and conditions of use: <http://www.tandfonline.com/page/terms-and-conditions>

This article may be used for research, teaching, and private study purposes. Any substantial or systematic reproduction, redistribution, reselling, loan, sub-licensing, systematic supply, or distribution in any form to anyone is expressly forbidden.

The publisher does not give any warranty express or implied or make any representation that the contents will be complete or accurate or up to date. The accuracy of any instructions, formulae, and drug doses should be independently verified with primary sources. The publisher shall not be liable for any loss, actions, claims, proceedings, demand, or costs or damages whatsoever or howsoever caused arising directly or indirectly in connection with or arising out of the use of this material.

# Torsional Buckling Behavior of SWCNTs Using a Molecular Structural Mechanics Approach Considering Vacancy Defects

VALI PARVANEH<sup>1</sup>, MAHMOUD SHARIATI<sup>2</sup>, HAMID TORABI<sup>3</sup> AND AMIR MASOOD MAJD SABETI<sup>2</sup>

<sup>1</sup>Department of Engineering, Islamic Azad University, Shahrood Branch, Shahrood, Iran

<sup>2</sup>Department of Mechanical Engineering, Shahrood University of Technology, Shahrood, Iran

<sup>3</sup>Young Researchers' Club, Mashhad Branch, Islamic Azad University, Mashhad, Iran

*In this paper, the influence of various vacancy defects on the critical buckling torques and twist angles in single-walled carbon nanotubes (SWCNTs) under torsional load is investigated using a new structural model built using the ABAQUS software. This model is a combination of other structural models and is designed to eliminate the deficiencies inherent in each of the individual approaches. For the first time, the effect of different types of vacancy defects on critical buckling torque and twist angle is studied for zigzag and armchair nanotubes of various lengths. The results show that vacancy defects have a considerable impact on the critical buckling torque. Moreover, zigzag nanotubes are found to be more sensitive to these defects than armchair nanotubes. The results obtained here are compared with those obtained using the continuum model, and reasonable agreement is observed.*

**Keywords** Structural mechanics approach, torsional buckling, single-walled carbon nanotubes, vacancy defects

## Introduction

Carbon nanotubes were first discovered by Iijima in 1991 (1) and, because of their particular mechanical and electrical features, have been investigated extensively by many researchers. A high Young's modulus and tensile strength combined with low density result in excellent mechanical properties for these structures (2–4). Experimental research in this context requires specially constructed laboratories and particular experimental conditions and is very expensive. Therefore, nonempirical modeling and simulation of these nanotubes have also been a focus of recent research. The computational methods commonly used for modeling of nanotubes are the *ab initio* method (5), the molecular dynamics (MD) method (4,6,7) and the tight binding method (8–10), which is a combination of the first two methods. These methods are computationally expensive, and therefore many researchers have turned to finite-element and continuum techniques. To solve the problems encountered with the experimental and atomic computational approaches just described, a

Address correspondence to Vali Parvaneh, Department of Mechanical Engineering, Islamic Azad University, Shahrood Branch, Shahrood, Iran. E-mail: vali.parvaneh@gmail.com

model with high accuracy and short run time is needed. Structural models solve the problems already mentioned; however, the available structural models are not comprehensive enough to meet research needs. In the models of Odegard et al. (11) and Meo and Rosi (12), torsion potentials were not considered. In the models of Li and Chou (13), Tserpes and Papanikos (14), Hu et al. (15) and Kalamkarov et al. (16), angle variation potential was modeled by beam bending. Although beam bending can be used to predict Young's modulus, it does not yield logical results for prediction of critical buckling loads because of improper modeling of the bending of C-C bonds.

In this paper, a new molecular structural mechanics approach using the ABAQUS software (17) is presented to study the torsional buckling behavior of SWCNTs. In general, existing research in this area is very limited.

Lu and Wang (18) investigated the buckling phenomenon in multi-walled carbon nanotubes (MWCNTs) under combined torque and axial loading, using three types of shell model to obtain the critical shear stress and the combined buckling mode. Their results showed that the critical shear stress and axial loading are dependent on the form of the axial loading and the type of MWCNT in such a way that, for identical MWCNTs, the critical shear stress under combined torque and axial tension loading is greater than that under combined torque and axial compression loading. Wang et al. (19) developed a continuum mechanics model for investigating the torsional buckling behavior of SWCNTs with different aspect ratios. The *material studio* commercial software package was used for molecular dynamic simulations to verify the buckling results. These simulations showed that the Donnell and Kromm models and the MD simulation predict almost the same twist angles. Yao and Han (20,21) examined nonlinear buckling and postbuckling behavior of single- and double-walled carbon nanotubes subjected to torsional load using a continuum mechanics elastic shell model. They used the boundary-layer theory of shell buckling and the singular perturbation technique to solve the governing equations based on Kromm-Donnell-type nonlinear differential equations. Their results demonstrate unstable postbuckling behavior for carbon nanotubes subjected to torsional load, with a longer postbuckling equilibrium path for thinner nanotubes than for thicker ones. They also calculated the critical buckling load for a carbon nanotube by comparing three pairs of values for Young's modulus ( $E$ ) and wall thickness ( $t$ ). The in-plane stiffness of SWCNTs was found to be an independent material parameter because the different values of  $E$  and  $t$  led to almost identical critical buckling loads. Wang (22) investigated the mechanical instability of double-walled carbon nanotubes subject to torsional motion using a molecular dynamics approach. He discovered a new mode shape for nanotubes under torsional loading, in which the inner tube shows a helically aligned buckling mode while the outer tube displays a local one-rim buckling mode similar to that of shorter nanotubes. Because the buckling modes of the constituent tubes have the same shapes, he concludes that continuum models are inapplicable. He then proposed a new concept of the equivalent thickness of double-walled carbon nanotubes, which enables the Kromm shell model to be used to derive the torsional buckling without the constraint of two tubes of identical shape.

Although torsional buckling of nanotubes has been investigated in previous studies, no guidelines are available for predicting the sensitivity and the amount of reduction of the torsion-load-carrying capacity of defective carbon nanotubes with respect to the buckling phenomenon. Therefore, the main objective of this paper is to investigate the torsional buckling behavior of carbon nanotubes using an atomistic modeling technique. In addition, the continuum shell model is also examined. This atomistic modeling technique is a molecular structural mechanics approach, which has been successfully used for the prediction of elastic axial buckling of carbon nanotubes under compressive load (23). Both perfect

and defective SWCNTs are considered in this paper, and the effects of different types of vacancy defects, nanotube aspect ratios, diameter and chirality on the critical buckling torque and twist angle are investigated.

## Carbon Nanotube Modeling

### *Existence of potentials in carbon nanotubes and interactions between atoms*

A SWCNT can be considered as a rolled graphene sheet in which the rotation direction determines the type of nanotube (i.e., zigzag, armchair, or chiral). Various interactions exist between the carbon atoms which comprise carbon nanotubes. The motions of the carbon atoms are regulated by a force field generated by electron-nucleus interactions and nucleus-nucleus interactions (24) expressed in the form of steric potential energy. The total steric potential energy is the sum of energies due to interactions between carbon atoms (25):

$$u_{total} = u_r + u_\theta + u_\phi + u_\omega + u_{vdw} + u_{el} \quad (1)$$

where  $u_r$ ,  $u_\theta$ ,  $u_\phi$  and  $u_\omega$  are the bond energies associated with bond stretching, angle variation or bond bending, dihedral angle torsion and out-of-plane torsion, respectively, while  $u_{vdw}$  and  $u_{el}$  are non-bonding energies associated with Van der Waals and electrostatic interactions, respectively. To predict the behavior of carbon nanotubes under axial tensional load, other potentials except for stretching and bending can be ignored. However, in buckling analysis, dihedral angles and out-of-plane potentials should be considered:

$$u_{total} = u_r + u_\theta + u_\phi + u_\omega \quad (2)$$

Various expressions have been developed for these potentials. The Brenner and Morse functions are well-known expressions for potentials which are applied mostly to nanotubes. The Brenner potential function is more accurate and versatile, but more complex than the Morse function.

In this paper, Morse potentials are employed for stretching and bending potentials, and a periodic type of bond torsion is applied for torsion interactions, as in equations (3–6). The parameters at these potentials are listed in Table 1 (26,27):

$$u_r = D_e \{ [1 - e^{-\beta(r-r_0)}]^2 - 1 \} \quad (3)$$

$$u_\theta = \frac{1}{2} k_\theta (\theta - \theta_0)^2 [1 + k_{sextic} (\theta - \theta_0)^4] \quad (4)$$

**Table 1**  
Parameters for molecular mechanics potentials

Interaction	Parameters
$u_r$	$D_e = 0.6031 \text{ nN}\cdot\text{nm}$ , $\beta = 26.25 \text{ nm}^{-1}$ , $r_0 = 0.142 \text{ nm}$
$u_\theta$	$k_\theta = 1.42 \text{ nN}\cdot\text{nm}/\text{Rad}^{-2}$ , $k_{sextic} = 0.754 \text{ Rad}^{-4}$ , $\theta_0 = 120^\circ$
$u_\phi$	$k_\phi = 0.278 \text{ nN}\cdot\text{nm}/\text{Rad}^{-2}$ , $n = 2$ , $\phi_0 = 180^\circ$
$u_\omega$	$k_\omega = 0.278 \text{ nN}\cdot\text{nm}/\text{Rad}^{-2}$ , $n = 2$ , $\omega_0 = 180^\circ$

$$u_\phi = \frac{1}{2}k_\phi [1 + \cos(n\phi - \phi_0)] \quad (5)$$

$$u_\omega = \frac{1}{2}k_\omega [1 + \cos(n\omega - \omega_0)] \quad (6)$$

As indicated in Figures 1(a) and 2, a nonlinear axial spring is used for modeling of the angle variation interaction between atoms. The relationship between changes in the bond and the corresponding change in length of the spring for small displacements can be expressed simply by equation (7) (11).

$$\Delta\theta \approx \frac{2(\Delta r)}{r_0}, r_0 = 0.142 \text{ nm} \quad (7)$$

Therefore, we can simplify equation (6) to equation (8):

$$u_\theta = \frac{2}{r_0^2}k_\theta (R - R_0)^2 \left[ 1 + \frac{16}{r_0^4}k_{\text{sextic}} (R - R_0)^4 \right] \quad (8)$$

The stretch force, the angle variation moment, the dihedral angle torque and out-of-plane torque can be obtained from differentiations of equations (3), (8), (5) and (6) as functions of bond stretch, bond angle, dihedral angle and out-of-plane angle variation, respectively:

$$F(r - r_0) = 2\beta D_e [1 - e^{-\beta(r-r_0)}] e^{-\beta(r-r_0)} \quad (9)$$

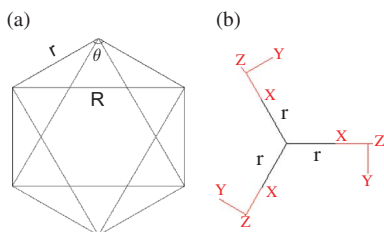


**Figure 1.** (a) A hexagonal unit cell, (b) location of local coordinates of each connector (color figure available online).

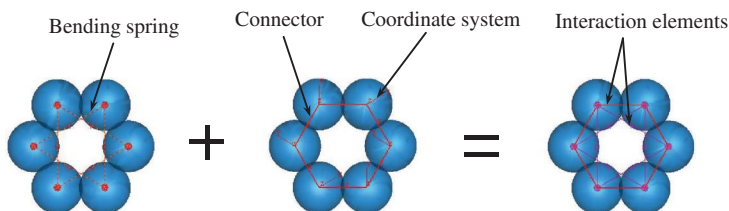


**Figure 2.** Spring and connector elements corresponding to the interactions of carbon atoms. (a) the angle variation interactions, (b) the stretching and torsional interactions, (c) total interactions (color figure available online).

$$F(R - R_0) = \frac{4}{r_0^2} k_\theta (R - R_0) \left[ 1 + \frac{16}{r_0^4} \left( 1 + \frac{4}{r_0^2} \right) k_{sexitic} (R - R_0)^4 \right] \quad (10)$$

$$T(\phi - \phi_0) = \frac{1}{2} k_\phi n \sin(n\phi - \phi_0) \quad (11)$$

$$T(\omega - \omega_0) = \frac{1}{2} k_\omega n \sin(n\omega - \omega_0) \quad (12)$$

### Construction of model in ABAQUS

In the present structural model, interactions between atoms are modeled with spring and connector elements so that the carbon atoms are joint points. A nonlinear connector is considered for modeling of the stretching and torsional interactions and a nonlinear spring for modeling of the angle variation interaction. Carbon atoms in ABAQUS are modeled by a discrete rigid sphere so that connector elements between atoms are adjoined to reference points at the center of the sphere (see Figure 1). A local coordinate is set at the center of each atom. This local coordinate is a combination of a Cartesian coordinate for stretching and a rotational coordinate for torsion. The X direction of these coordinates is in the connector direction, and the Z direction is vertical to the central axis of the nanotube. Because we can only use a linear spring in the CAE space of ABAQUS, by changing the linear spring command to a nonlinear spring command in the input file and by applying the nonlinear data for  $F(\Delta R)$  versus  $\Delta R$  using equation (10), we can apply the bond bending spring to the model. For applying bond stretch and torsion forces to the connectors, we can apply the nonlinear stiffness in three directions (X,Y,Z) directly. For stretching stiffness in the X direction, we can obtain the nonlinear data for  $F(\Delta r)$  versus  $\Delta r$  by Eq. 9, and for torsional stiffness in X direction we can obtain the nonlinear data for  $T(\Delta\phi)$  versus  $\Delta\phi$  by equation (11). For torsional stiffness in the Y direction, we can obtain the nonlinear data for  $T(\Delta\omega)$  versus  $\Delta\omega$  by equation (12).

## Results and Discussion

### Torsional buckling of perfect SWCNTs

The critical buckling torques and twist angles of perfect zigzag and armchair carbon nanotubes have been predicted by the present structural model. Figure 3 shows the critical buckling torques and twist angles for different nanotube lengths and diameters. Increasing the length of nanotube results in a decrease in the critical buckling torque and an increase in the critical twist angle. This shows that the critical buckling torque in shorter nanotubes is more sensitive to changes in length. Furthermore, as the diameter increases, the critical torque also increases while the critical twist angle decreases. The effect of the chirality of the tube on the critical buckling torque is significant when  $\frac{L}{D} < 5$ . The critical twist angles of zigzag CNTs with  $\frac{L}{D} > 2$  are much greater than those of armchair CNTs. It is worth mentioning that the results obtained from the present model for zigzag (16,0) CNTs are in good agreement with those obtained from MD simulation (22). Figure 4 presents the buckling mode shapes of (7,7) CNTs of different lengths under torsional buckling load. It can be seen that for short CNTs, increasing the length of the nanotube decreases the number of waves.

In Figure 5, the results of the present model can be seen to be in good agreement with those of the simple continuum model when an effective thickness value of 0.066 nm is used

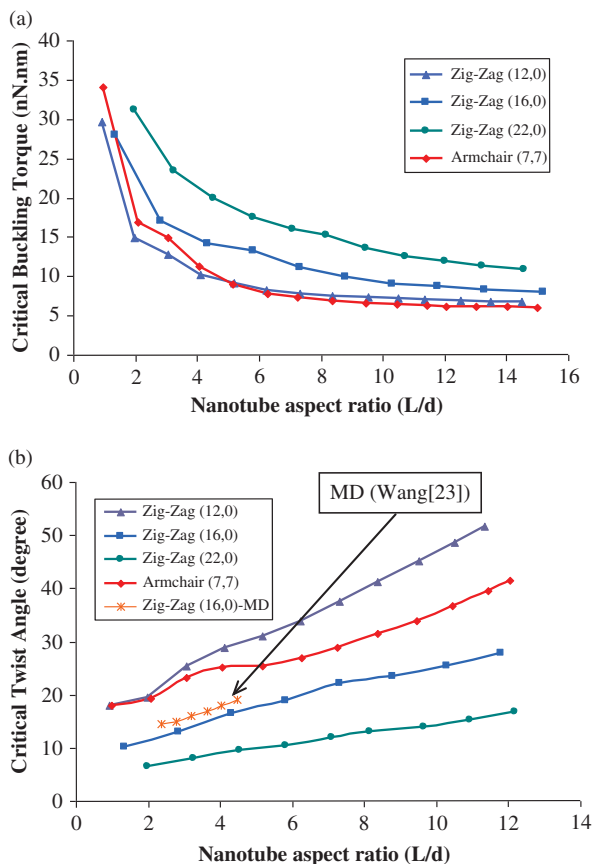


**Figure 3.** Influence of the length and diameter of SWCNTs on (a) critical buckling torque and (b) critical twist angle (color figure available online).

for the nanotube (28). For long nanotubes, the agreement between the results from the two models is better than for short ones.

The buckling mode shapes obtained from displacement counters for (12,0), (16,0) and (22,0) CNTs are compared with those obtained using the continuum model, as shown in Figure 6. With increasing diameter, shell buckling appears in the form of two, three or four waves in the circumferential direction.

### *Torsional buckling of defective SWCNTs*

The types of vacancy defects encountered in carbon nanotubes are illustrated in Figure 7. The defects studied include single, two-opposite, double and triple vacancies.

In the remaining figures, the buckling torque is normalized using the buckling torque multiplier ( $k$ ), which is defined as follows:

$$k = \frac{T_d}{T_p} \quad (7)$$

where  $T_p$  and  $T_d$  are the critical torsional buckling values for perfect and defective nanotubes, respectively. Normalized critical buckling torques for two types of nanotubes,

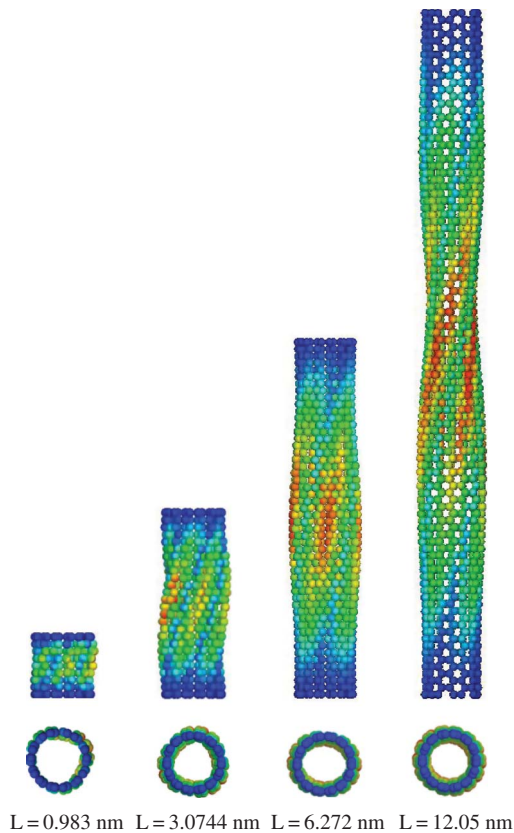


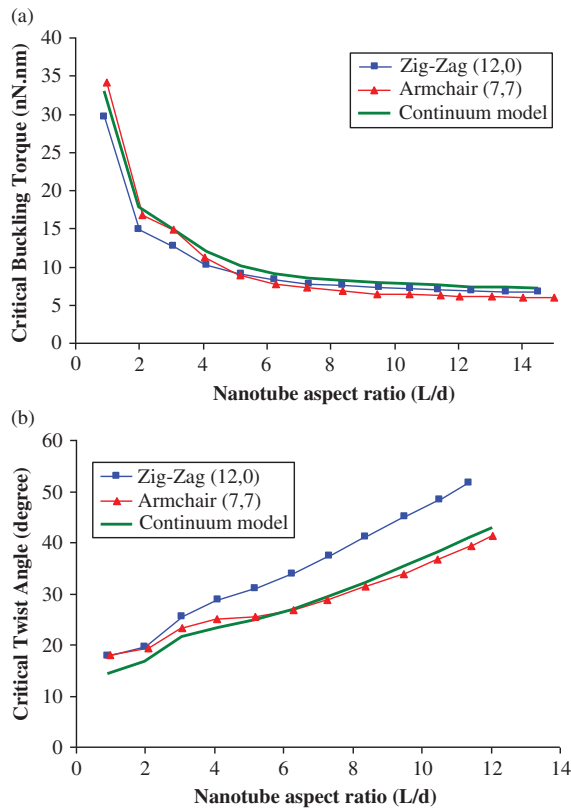
**Figure 4.** Mode shapes of (7,7) SWCNTs under torsional torque for various lengths (color figure available online).

armchair and zigzag, are shown in Figure 8, where various types of defects based on different nanotube lengths are compared. As shown in Figure 8, triple vacancies contribute mostly to lessening the critical buckling torque, while the most modest effects are seen for single vacancies. In addition, double and two-opposite vacancies operate similarly in these types of nanotubes. As nanotube length increases, the effects of defects diminish gradually. This phenomenon occurs earlier in armchair nanotubes than in zigzag ones.

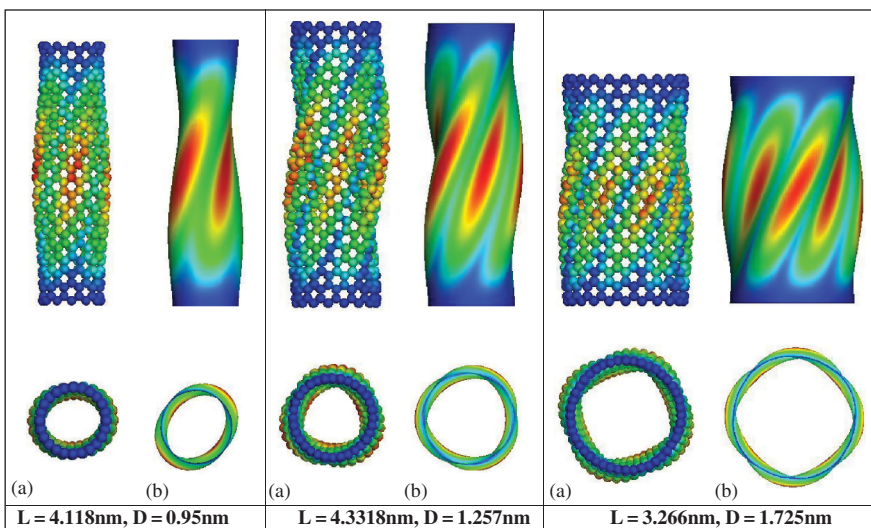
A comparison of the effects of defects in nanotubes and those of a cutout in the continuum model has also been performed. The creation of a cutout in the continuum model is represented by a reduction of nanotube area. To obtain agreement between the created cutout and each defect type, various cutout angles, as shown in Figure 9, are considered for the corresponding continuum model for armchair and zigzag nanotubes; the results of this comparison are shown in Figure 10. This variation in angle leads to good agreement between the two models, which is enhanced as nanotube length increases.

Figure 11 illustrates the mode shapes of defective nanotubes with single and two-opposite vacancies in the middle of the nanotubes. It can be seen that the mode shapes of defective nanotubes under torsion are similar to those of the continuum model with a cutout.





**Figure 5.** Comparison of the results of the present model with those of the continuum model for (a) critical buckling torque and (b) critical twist angle (color figure available online).



**Figure 6.** (a) Mode shapes from the present model, (b) mode shapes of perfect nanotubes from the continuum model (color figure available online).

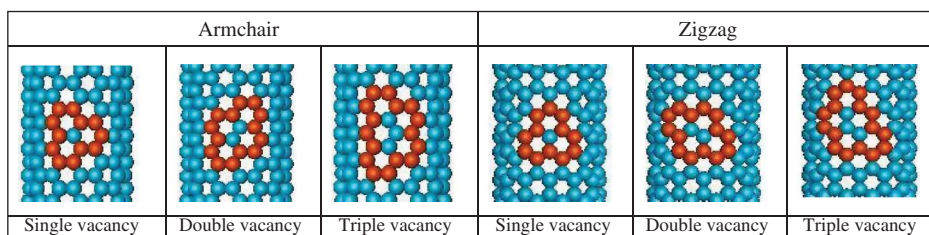


**Figure 7.** Schematic view of vacancy defects in carbon nanotubes (color figure available online).

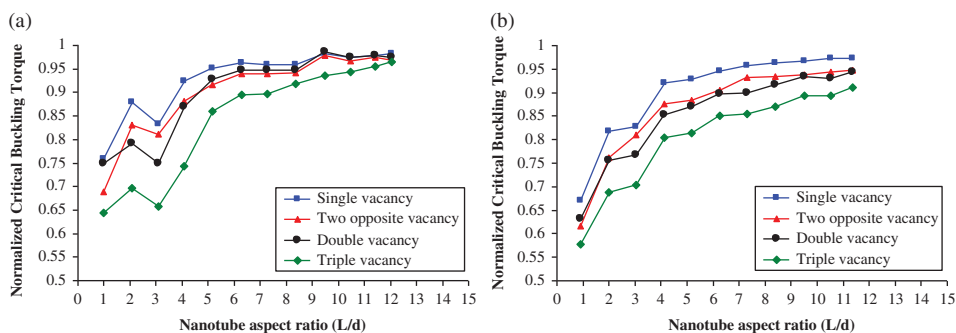


**Figure 8.** Normalized critical buckling torques as a function of tube length for defective SWCNTs: (a) armchair, (b) zigzag (color figure available online).

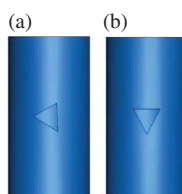


**Figure 9.** Cutouts created in the continuum model: (a) cutout of a single vacancy based on the corresponding armchair nanotube; (b) cutout of a single vacancy based on the corresponding zigzag nanotube (color figure available online).

## Conclusions

In this paper, SWCNTs and the effects of vacancy defect types on their buckling behavior under torsion have been studied by means of a structural mechanics approach using ABAQUS. From these investigations, the following results can be concluded:

1. For nanotubes of similar diameter, the value of the critical buckling torque is approximately equal for armchair and zigzag nanotubes.
2. With increasing nanotube diameter, the critical buckling torques converge to a finite value, while the critical twist angles diverge.
3. In armchair and zigzag nanotubes, the values of the critical twist angle are similar for tubes of relatively short length; however, these values diverge as the length increases.

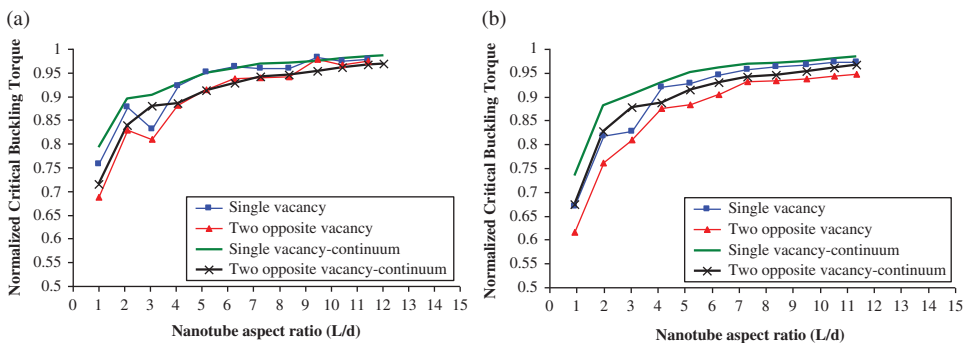


**Figure 10.** Comparison of the results of the present model with those of the continuum model for defective SWCNTs: (a) armchair, (b) zigzag (color figure available online).

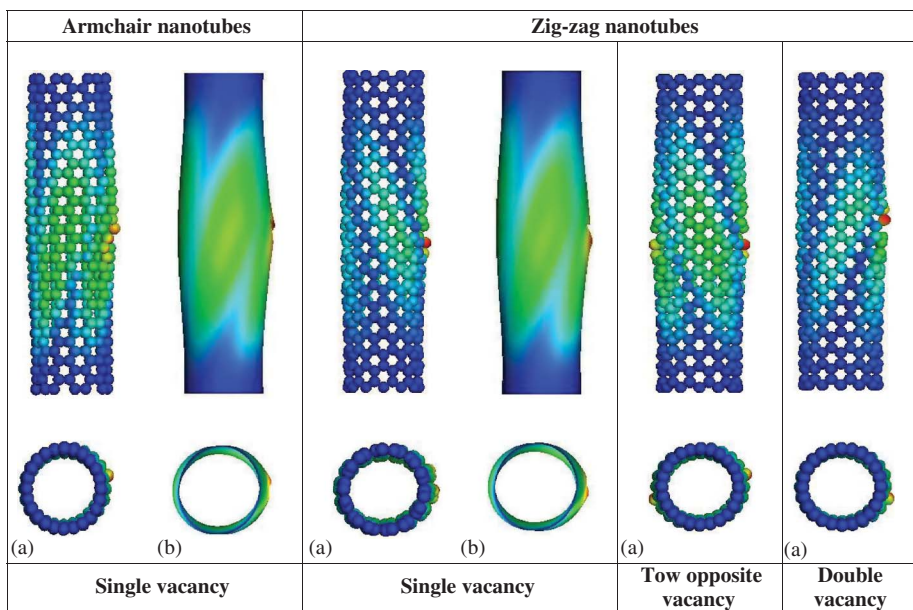


**Figure 11.** (a) Mode shapes from the present model, (b) mode shapes from the continuum model for defective CNTs (color figure available online).

- Critical torque values as calculated by the present model agree well with those calculated by the continuum model; therefore, the continuum model can be used to estimate the critical buckling torque of armchair and zigzag SWCNTs.
- In short nanotubes, the decrease in the critical buckling torque of defective SWCNTs becomes considerable as the vacancy defects become longer.
- Triple vacancies contribute substantially to reducing the critical buckling torque, while single vacancies have only a modest effect.
- Double and two-opposite vacancies operate similarly in the two types of CNTs.
- We can most likely model the defective SWCNTs by cylindrical shells with a cutout due to the similarity between their buckling behaviors.

## References

1. Iijima, S. (1991) Helical microtubes of graphitic carbon. *Nature*, 354: 56–58.
2. Dresselhaus, M. S., Dresselhaus, G., and Eklund, P. C. (1996) *Science of Fullerenes, Carbon Nanotubes*. Academic Press: San Diego.
3. Nardelli, M. B., Fattbert, J. L., Orlikowski, D., Roland, C., Zhao, Q., and Bernholc, J. (2000) Mechanical properties, defects and electronic behavior of carbon nanotubes. *Carbon*, 38: 1703–1711.
4. Yakobson, B. I., Brabec, C. J., and Bernholc, J. (1996) Nanomechanics of carbon tubes: Instability beyond linear response. *Phys. Rev. Lett.*, 76: 2511–2514.
5. Kudin, K. N., Scuseria, G. E., and Yakobson, B. I. (2001) C<sub>2</sub>F, BN and C nanoshell elasticity from ab initio computations. *Phys. Rev. B*, 64: 235406.
6. Lu, J. P. (1997) Elastic properties of carbon nanotubes and nanoropes. *Phys. Rev. Lett.*, 79: 1297–1300.
7. Overney, G., Zhong, W., and Tomanek, D. (1993) Structural rigidity and low-frequency vibrational modes of long carbon tubules. *Zeitschrift für Physik D*, 27: 93–96.
8. Goze, C., Vaccarini, L., Henrard, L., Bernier, P., Hernandez, E., and Rubio, A. (1999) Elastic and mechanical properties of carbon nanotubes. *Synth. Met.*, 103: 2500–2501.
9. Hernandez, E., Goze, C., Bernier, P., and Rubio, A. (1998) Elastic properties of C and B<sub>x</sub>C<sub>y</sub>N<sub>z</sub> composite nanotubes. *Phys. Rev. Lett.*, 80: 4502–4505.
10. Molina, J. M., Savinsky, S. S., and Khokhriakov, N. V. (1996) A tight-binding model for calculations of structures and properties of graphitic nanotubes. *J. Chem. Phys.*, 104: 4652–4656.
11. Odegard, G. M., Gates, T. S., Nicholson, L. M., and Wise, K. E. (2002) Equivalent-continuum modeling with application to carbon nanotubes. NASA/TM-211454.
12. Meo, M. and Rossi, M. (2006) Tensile failure prediction of single-walled carbon nanotube. *Eng. Frac. Mech.*, 73: 2589–2599.
13. Li, C. Y. and Chou, T. S. (2003) A structural mechanics approach for the analysis of carbon nanotubes. *Int. J. Sol. Struc.*, 40: 2487–2499.
14. Tserpes, K. I. and Papanikos, P. (2005) Finite element modeling of single-walled carbon nanotubes. *Composites: Part B*, 36: 468–477.
15. Hu, N., Fukunaga, H., Lu, C., Kameyama, M., and Yan, B. (2005) Prediction of elastic properties of carbon nanotube-reinforced composites. *Proceed. Roy. Soci. Lon. A. Math. Phys. Sci.*, 461: 1685–1710.
16. Kalamkarov, A. L., Georgiades, A. V., Rokkam, S. K., Veedu, V. P., and Ghasemi-Nejhad, M. N. (2006) Analytical and numerical techniques to predict carbon nanotubes properties. *Int. J. Sol. Struc.*, 43: 6832–6854.
17. ABAQUS (2006) ABAQUS 6.6 User's Manual, Hibbit, Karlson and Sorenson, Inc.
18. Lu, Y. J. and Wang, X. (2006) Combined torsional buckling of multi-walled carbon nanotubes. *J. Phys. D: App. Phys.*, 39: 3380–3387.
19. Wang, Q., Quek, S. T., and Varadan, V. K. (2007) Torsional buckling of carbon nanotubes. *Phys. Lett. A*, 367: 135–139.
20. Yao, X. and Han, Q. (2008a) A continuum mechanics nonlinear postbuckling analysis for single-walled carbon nanotubes under torque. *Euro. J. Mech. A/Sol.*, 27: 796–807.
21. Yao, X. and Han, Q. (2008b) Torsional buckling and postbuckling equilibrium path of double-walled carbon nanotubes. *Compos. Sci. Tech.*, 68: 113–120.
22. Wang, Q. (2008) Torsional buckling of double-walled carbon nanotubes. *Carbon*, 46: 1159–1174.
23. Parvaneh, V., Shariati, M., and Majd Sabeti, A. M. (2009) Investigation of vacancy defects effects on the buckling behavior of SWCNTs via a structural mechanics approach. *Euro. J. Mech-A/Solids*, 28: 1072–1078.
24. Machida, K. (1999) *Principles of Molecular Mechanics*, Kodansha and John Wiley & Sons Co-publication: Tokyo.

25. Rappe, A. K., Casewit, C. J., Colwell, K. S., Goddard III, W. A., and Skiff, W. M. (1992) UFF, A full periodic-table force-field for molecular mechanics and molecular dynamics simulations. *J. Amer. Chem. Soc.*, 114: 10024–10035.
26. Belytschko, T., Xiao, S. P., Schatz, G. C., and Ruoff, R. S. (2002) Atomistic simulations of nanotube fracture. *Phys. Rev. B.*, 65: 235–430.
27. Cornell, W. D., Cieplak, P., Bayly, C. I., Gould, I. R., Merz, K. M., Ferguson, D. M., Spellmeyer, D. C., Fox, T., Caldwell, J. W., Kollman, P. A. (1995) A second generation force-field for the simulation of proteins, nucleic-acids, and organic-molecules. *J. Amer. Chem. Soc.*, 117: 5179–5197.
28. Yakobson, B. I. and Avouris, P. (2001) Mechanical properties of carbon nanotubes. In *Carbon Nanotubes, Topics in Applied Physics, Vol. 80*; Dresselhaus, M. S., Dresselhaus, G., and Avouris, P. (eds.), Springer Verlag: Berlin/Heidelberg, pp. 287–329.